Wind-Tunnel Interference Effects on Delta Wing Aerodynamics Computational Fluid Dynamics Investigation

M. R. Allan,[*] K. J. Badcock,[†] G. N. Barakos,[‡] and B. E. Richards[§]
University of Glasgow, Glasgow, Scotland G12 8QQ, United Kingdom

Abstract
Reynolds averaged Navier–Stokes simulations of a static and pitching delta wing within three wind tunnels havebeen performed. These simulations have been compared with the case of the wing in free air to ascertain the various influences of the walls on the vortical flow. The presence of tunnel walls has been found to promote vortex breakdown, with side wall proximity being the dominant factor. Roof and floor proximity has been seen to have a negligible effect on vortex breakdown. During pitching motion, side wall proximity delays vortex reformation after breakdown has reached its most upstream location, during cyclic pitching motion. This delay is recovered onthe upstroke of the motion. These results confirm previous work with Euler simulations of tunnel interference.

Introduction

IND tunnels are used to test the aerodynamic characteristics of aircraft, and the influence of the tunnel walls must be taken into account when considering test results. Historically, wind-tunnel corrections have been based on linear potential flow theory.[1] To obtain good quality and reliable test data, factors relat- ing to wall interference, flow angularity, local variations in velocity, and support interference must be taken into account. Karou[2] found

Re = Reynolds number, ρU_∞

Clearly, the flow conditions within a wind tunnel will be different from those a wing would experience in free air. The interactions between the wing and wall flowfields induce longitudinal and lat- eral variations (streamline curvature and aerodynamic twist, respec- tively) to the freestream, in addition to those attributed to the wing alone. These differences may result in a reduction in the average downwash experienced by the model, a change in the streamline curvature about the model, an alteration to the local angle of attackalong the span of the model, and changes in dynamic pressure about the model due to solid and wake blockage and in the buoyancy effect due to the axial pressure gradient along the tunnel test section. The magnitude of these effects increases with model size (increasing solid blockage).

Weinberg[4] conducted an experimental investigation into wall ef- fects. Two sets of three wings were tested (one set with 60-deg sweep and one set with 70-deg sweep), each wing with a different span size. The experiment was performed in a square water tunnel(low Reynolds-number) at a constant flow velocity of 11 m/s. Thetunnel size was 45 45 cm. He found that for the three wings with 70-deg sweep, as the wing size was increased and at a constant an- gle of attack, vortex breakdown moved downstream. For the three wings with 60-deg sweep, he found that, as the wing span-to-tunnel width ratio increased from 0.175 to 0.35, the wall effects followed similar trends, that is, vortex breakdown was shifted downstream with increasing wing size. However, when the wing span-to-tunnel width ratio was increased from 0.35 to 0.7, no significant change was observed. This suggested that effective camber was not the onlyinfluence. For both the 60- and the 70-deg wings, the difference inbreakdown location observed from the smallest model to the largest model was of the order $25\% c_r$.

Thompson and Nelson[5] investigated experimentally the influence of tunnel walls on a 70-deg delta wing by testing full-, two-thirds-, and half-scale models in a square tunnel. (The largest model gave the ratios b/H b/W 0.364.) Because of a steady hysteresis ef- fect, the wing was tested for a quasi-steady upward stroke and a downward stroke. It was found that for the smallest model tested (b/H b/W 0.124) the breakdown location shifted downstream by as much as $15\% c_r$ on both the quasi-steady upstroke and down- stroke. For the half-scale model and the full-scale model, there ap- peared to be little difference in the breakdown locations. As stated by Thompson and Nelson, this shift downstream as model size is decreased is in contrast to the results of Weinberg.[4] Weinberg used a Reynolds number an order of magnitude lower, and a constant velocity, as opposed to keeping the Reynolds number constant (as in the experiments of Thompson and Nelson). The vortex suction on the model surface increased with model size.

More recently, Pelletier and Nelson[6] studied the effect of tunnel interference on 70-deg delta wings. Experiments were conducted ina water tunnel with three different sized wings. These low Reynolds number tests agreed with the previous findings of Thompson and Nelson,[5] who tested at higher Reynolds number, in that breakdown moved toward the apex with increasing wing size. Pelletier and Nelson used the method of images to explain this effect, concluding that the tunnel walls increased the mean incidence of the wing, thus, promoting breakdown.

Verhaagen et al.[7] performed Euler calculations of the flow overa 76-deg delta wing inside wind tunnels of increasing size. The wing span-to-tunnel width ratios considered were 0.292, 0.389, and0.584, and the test section was octagonal. To model the effect of a secondary separation, a small fence was placed where secondary separation would occur. It was found that decreasing the tunnel size (increasing the wing span-to-tunnel width ratio) increased thesuction in the vortices and increased the velocities in the vortex core, due to an increase in circulation with decreasing tunnel size.

Mitchell[8] tested a at upper and lower surface 70-deg delta wing at 27-deg angle of attack in the ONERA S2Ch and ONERA F2 tunnels. The tests had model span-to-tunnel width ratios of 0.23 and 0.49, respectively. It was found that the mean location of breakdown was upstream (around $7\% c_r$) in the narrower ONERA F2 tunnel in comparison to the larger ONERA S2Ch tunnel.

Allan et al.[9] performed Euler simulations of tunnel interference effects on a 65-deg delta wing in various tunnels for static and pitching cases. It was observed that tunnel side walls were the most influential factor on breakdown location with roof and floor having little effect. It was also noted that in pitching simulations the tunnel interference effects were strongest on the downstroke, during the vortex reformation.

Allan et al.[10] performed Reynolds averaged Navier–Stokes RANS simulations of a 70-deg delta wing in a wind tunnel, with and with- out downstream support structures. It was found that the level of support structure interference was heavily dependent on whether or not the vortex cores impinged on the support. Using tunnel cen- terline supports with small models may promote vortex breakdown, with breakdown moving downstream as the model size increases (as the core trajectory moves away from the centerline and interferenceregion).

It is the aim of this work to confirm the previous Euler results and suggest best practices for tunnel testing of delta wings.

Flow Solver

All simulations described in this paper were performed using the University of Glasgow parallel multiblock (PMB) Reynolds averaged Navier–Stokes (RANS) solver. A full discussion of the code and turbulence models implemented is given in Ref. 11. PMB

uses a cell-centered finite volume technique to solve the Euler and RANS equations. The diffusive terms are discretized using a central differencing scheme, and the convective terms use Roe's scheme with MUSCL interpolation offering third-order accuracy. Steady flow calculations proceed in two parts, initially running an explicit scheme to smooth out the flow solution, then switching to an implicit scheme to obtain faster convergence. The preconditioning is based on block incomplete lower–upper factorization and is also decou- pled between blocks to increase the parallel performance. The linear system arising at each implicit step is solved using a generalized con- jugate gradient method. For time-accurate simulations, Jameson's pseudotime (dual-time stepping) formulation[12] is applied, with the steady-state solver used to calculate the pseudosteady states at each physical time step.

The RANS equations are solved, and the two-equation k–ω turbu- lence model is used for closure. It is well known that most linear two- equation turbulence models overpredict the eddy viscosity within vortex cores, thus, causing too much diffusion of vorticity.[13] This weakens the strength of the vortices and can eliminate secondary vortices, especially at low angles of attack, where the vortices are already weak. The modification suggested by Brandsma et al.[14] was, therefore, applied to the standard k–ω model of Wilcox[15] to reduce the eddy viscosity in vortex cores, by limiting the production of turbulent kinetic energy k, as

$$P_k = \min\left(P^u, (2.0 + 2.0 \min\{0, r - 1\})\rho\beta^* k\omega\right) \quad (1)$$

Here P^u is the unlimited production of k and r is the ratio of the magnitude of the rate of strain and vorticity tensors. When k is over- predicted in the vortex core, it will be limited to a value relative to the dissipation in that region. After comparison with experiment,[14,16,17] this modification was found to improve predictions compared with the standard k–ω turbulence model and is, therefore, used in all simulations presented.

The Computational Fluid Dynamics Laboratory at the Univer- sity of Glasgow owns a cluster of personal computers. The clus- ter is known collectively as Jupiter and is fully described by Badcock et al.[18] The cluster used for this study has 32 nodes of 750-MHz AMD Athlon Thunderbird uniprocessor machines, each with 768 MB of 100-MHz dynamic random access memory (DRAM). Message passing interface (MPI) is used to link up multi- ple nodes to create a virtual machine, which is used to execute com- putationally demanding problems. PMB balances the node loadings (number of cells per node) by spreading the blocks over all of the nodes of the virtual machine. Halo cell values are passed between adjacent blocks using MPI.

Test Cases

The wing used for all work described is that of the WEAG-TA15WB1 65-deg sweep delta wing. The WEAG-TA15 WB1 model (Fig. 1) was tested at DLR, German Aerospace Research Center, Braunschweig, Germany, by Löser.[19] Experiments were carried out at two freestream Mach numbers (0.06 and 0.12) with Reynolds numbers based on the root chord of $1.55\ 10^6$ and $3.1\ 10^6$. The experiments were carried out in the 2.85 3.2 m low-speed atmo- spheric wind tunnel (NWB) of DNW, located at DLR Braunschweig, using the open test section.

The wind-tunnel model had an inner chord of 1200 mm, a tip chord of 180 mm, and a leading edge sweep of 65 deg. The model is fully symmetric with a sharp leading edge, which has a radius of

0.25 mm. The aerofoil consists of an arc segment from the leading edge to 40% of the local chord, the region 40%–75% of the local chord is defined by the NACA 64A005 aerofoil, and from 75% of the local chord to the trailing edge the aerofoil is a straight line inclined at 3 deg. The wind-tunnel model has a fuselage of 160 mm diameter built into the lower surface of the wing, though this is not expected to influence the upper surface flow. The fuselage was not modeled in the current work.

The computational test cases in Table 1 were considered. Four boundary conditions were specified relating to free air and in-tunnel situations. The first case was that of far-field conditions specified at the outer boundaries with all boundaries being $10c_r$ from the wing.

the 3 3 to the 2 3 tunnel. Again, as seen in Euler solutions, there is a clear vortical flow pattern on the side wall downstream of the wing's trailing edge. This vortical flow pattern extends the length of the tunnel. The vortical flow pattern on the side walls is observed for the three tunnels, reducing in extent with decreasing b/W ratio.[21] It is clear that the close proximity of the 2 3 tunnel side wall induces the largest favorable pressure gradient, which indicates that the side wall produces the most detrimental interference.

To assess the adverse pressure gradient experienced by the vortex core in the tunnels, the pressure distribution along the leading-edge vortex core is shown in Fig. 8. As the vortex is placed within tun- nel constraints, it can be seen that the suction in the vortex core increases, with the largest increment being observed in the 2 3 tunnel, where the maximum suction is around 15% greater than that for the far-field solution. The 3 3 and 3 2 tunnels produce a sim- ilar increment in suction (of around 6% in comparison to that of the far-field solution). This increase induces a stronger adverse pressure gradient, as seen in Fig. 8, thus, promoting vortex breakdown.

The flow angles (the angle at which the flow is deflected due to the presence of the wing) at the 2 3 tunnel side wall location are shown in Fig. 9. As in the Euler results (see Ref. 9), it can be seen that the presence of the side walls has increased the flow angles along the wing, thus, increasing the mean effective incidence of the

the effect of increasing blockage is to increment the lift and drag, the vortex lift contribution (recalling Polhamus's suction analogy[24]) becomes a lower percentage of the total lift. Therefore, when the blockage is increased and the potential lift component becomes larger, the hysteresis due to vortex lift contribution becomes less apparent. If we compare against Euler solutions (see Ref. 9), where the vortices are closer to the surface and, therefore, the vortex lift is higher, the effect of the increase in potential lift on the hysteresis loop width is lower. Also because the vortices are closer to the wing in the Euler solutions, an increase in vortex strength, that is, as incidence or b/W ratio increases, will be more apparent on the suction peaks (and, therefore, the vortex lift) in comparison to the RANS solutions.

The pitching moment curves provide a good measure of how much the flow structure varies at a given point in the pitching cy- cle due to tunnel wall constraints. Because breakdown locations are unavailable once breakdown has passed the trailing edge (due to the grid density decreasing in that region), the pitching moment curves provide a great deal of insight as to how the tunnel walls are influencing the flow at the low incidences, being sensitive to longitudinal flow variations. The understanding of the side wall in- fluences on breakdown location gained from the steady results, and the effect that blockage has on the loads and moments, allows a great deal of information to be interpreted solely from the pitch- ing moment curves. Figure 16 shows the pitching moment curves obtained from each solution. Clearly the smallest difference is in the angle of attack range 15–21 deg on the upstroke of the pitch- ing motion. When it is recalled that the blockage in the 2 3 and

3 × 2 tunnels is similar (which will have an effect on the pitch- ing moment), it can be concluded that, because the pitching mo- ment curves in the 2 × 3 and 3 × 2 tunnels are almost identical in the low incidence range, the tunnel side walls have a lesser influ- ence on the vortices. Also note that wind-tunnel wall interference will depend heavily on vortex strength, which increases with inci- dence. (The mirror images strengthen as the leading edge vortices strengthen.) Thus, we would expect the greatest interference to oc- cur at high incidence. It can, therefore, be assumed that, at low incidence, the difference between the 2 × 3 and 3 × 2 tunnel curves, and those from the 3 3 and far-field solutions, is purely due to blockage.

As the incidence is increased and the influence of the tunnel side walls increases, the effect of the promotion of vortex breakdown crossing the trailing edge early in the 2 × 3 tunnel can be seen at around 22 deg on the upstroke. Because the breakdown forms just past the trailing edge, there is a slight increase in the nose down pitching moment due to the breakdown region acting like a bluff body in the CFD solutions. (A small suction peak is observed on the wing surface beneath the vortex breakdown region.) This provides additional suction near the trailing edge, increasing the nose down pitching moment slightly. As the incidence increases further and breakdown moves completely onto the wing, a loss of the nose down pitching moment occurs as expected. (This occurs earliest in the 2 × 3 tunnel at around 24.5 deg.) The solutions from the other two tunnels and the far-field solution follow a similar pattern, although this occurs later in the pitching cycle. At around 25 deg, it is evident that vortex breakdown is well established over the wing in all of the solutions (Fig. 17), which is highlighted by a sharp decrease in the nose down pitching moment.

Now consider only the 2 × 3 tunnel pitching moment curve: It can be seen that from 27 deg to around 25 deg on the down- stroke that the pitching moment remains relatively constant. In this region, vortex breakdown is held at its most upstream loca- tion (Fig. 17 for confirmation) due to the increased influence of the tunnel walls at high incidence, which are promoting vortex breakdown. It can be concluded that, as in Euler simulations (see Ref. 9), there is a delay in vortex recovery. From around 25 to 22 deg, it is observed that the 2 × 3 tunnel solution tends toward that of the other tunnels, due to the reducing tunnel interference. From around 22 deg downward, it can be seen that the pitching moment curves from all tunnels follow a similar trend to that of the far-field solution as the tunnel interference decreases. Most

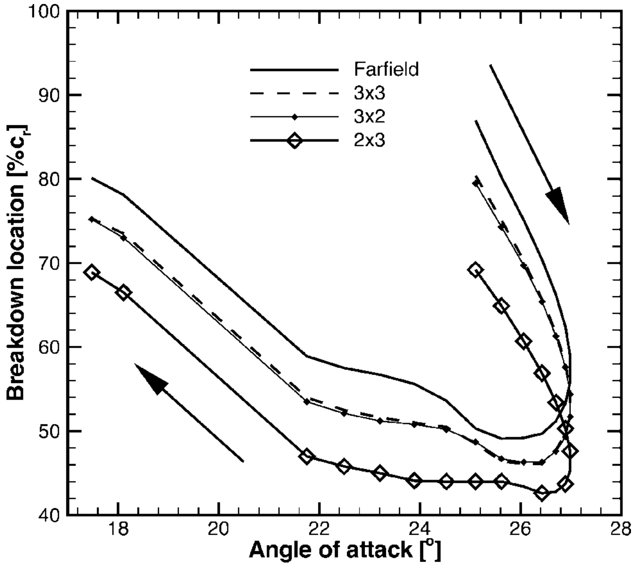

Fig. 17 WEAG-TA15 wing, unsteady breakdown locations for sinu- soidal pitching motion.

attention has been paid to the 2 × 3 tunnel solution: however, it is also clear that the 3 × 3 and 3 × 2 tunnels have influenced the curves, both in blockage terms and from a slight promotion of vortex breakdown.

The vortex breakdown locations for the RANS pitching calcu- lations are given in Fig. 17. Only locations at which breakdown is over the wing are shown. Downstream of the trailing edge, the grid coarsens, and as such, breakdown locations cannot be obtained in this region. Note that on the upstroke the vortex breakdown loca- tion has been taken where the axial component of velocity becomes zero. However, on the downstroke of the motion where vortex break- down is moving downstream, it is not possible to use this criterion for breakdown because the motion of the breakdown location pro- hibits this. (The axial velocity does not become zero.) As such, for the downstroke the breakdown location was defined as the location where the turbulent Reynolds number (or equally the eddy viscos- ity) increases rapidly. A turbulence Reynolds number of near 600.0 (where eddy viscosity is 600 times greater than the molecular vis- cosity) was chosen as the breakdown location, which corresponded well with where the axial velocity was observed to become zero on the upstroke. As the wing pitches up, the breakdown clearly moves upstream in a near linear manner, reaching its most upstream value at around 26 deg on the downstroke. In the 2 × 3 tunnel, in particu- lar, it can be seen that the breakdown is held near its most upstream location until around 24 deg on the downstroke. This is because the tendency of the side walls is to promote vortex breakdown; thus, at the high incidence, the effect of the side walls is strong and, therefore, breakdown is held upstream. When the remainder of the downstroke is considered, as the wing pitches down it can be seen from the pitching moment curves that there is still a wide variation in pitching moment between the various solutions. This indicates that the tunnel effects are large on the downstroke of the motion because breakdown will remain over the wing for longer as the wing leaves a state of high tunnel interference. A similar trend was observed with Euler simulations (see Ref. 9).

To visualize the extent of the interference with incidence, the tunnel wall pressure distributions for the 2 × 3 tunnel are given in Fig. 18. The side wall interference is clearest in the solutions from the 2 × 3 tunnel, although the discussion applies to the other tunnels. As the wing pitches up and the vortices become stronger, we see a much stronger interference pattern on the side walls. It is this strong interference at high incidence that causes the delay in vortex recovery in the 2 × 3 tunnel. The effect of blockage can also be seen as a high pressure beneath the wing, increasing with frontal area blockage and incidence.

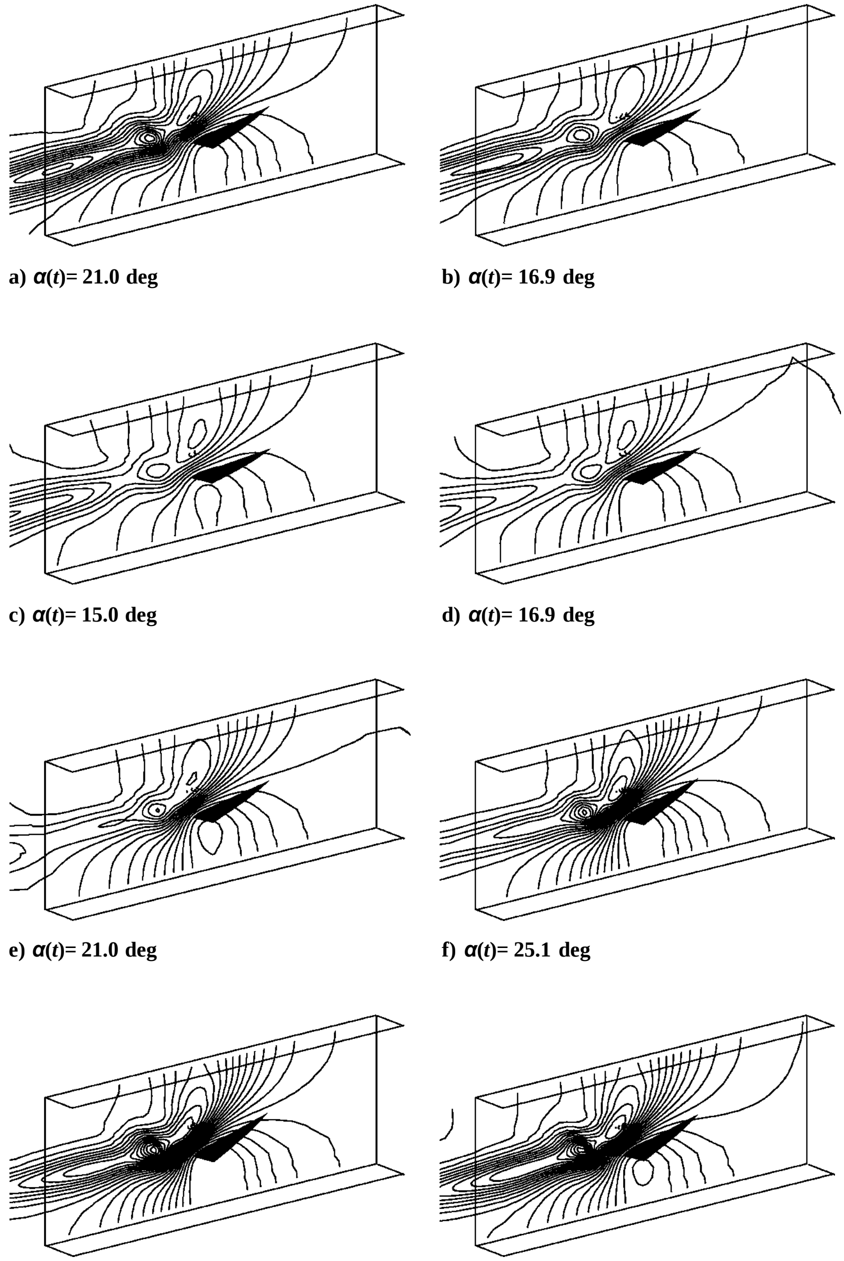

a) $\alpha(t)$= 21.0 deg b) $\alpha(t)$= 16.9 deg

c) $\alpha(t)$= 15.0 deg d) $\alpha(t)$= 16.9 deg

e) $\alpha(t)$= 21.0 deg f) $\alpha(t)$= 25.1 deg

g) $\alpha(t)$= 27.0 deg h) $\alpha(t)$= 25.1 deg

Fig. 18 Tunnel wall surface pressures during sinusoidal pitching.

Conclusions

Aerodynamic impacts of wind tunnel wall limitations on delta wings were studied. According to the results of the research,
1) The simulations show that the leeward surface flow over delta wings may be accurately modeled by using the RANS equations.
2) Recent simulations have shown that the side walls play a more significant role than the wingtips in the wind-tunnel interference experienced by delta wings. Hence, models should be positioned such that their sides are at a maximum distance from the walls.

The existence of the roof and floor has less of an effect on vortex collapse than side walls, according to the simulations.
4) The closeness to the side walls continually enhances the disintegration of the vortex.
5) In tunnels, as opposed to free-air situations, the vorticity is distributed differently across the whole vortex. Parameters like pitching moment may be particularly challenging to adjust by supposing a shift in mean effective incidence alone.
Six) The degree to which the breakdown varies for sinusoidal pitching motion depends on where the wing is in the pitching cycle.
7) The pace at which a vortex collapses is strongly affected by the proximity of the walls on either side, more so during the downstroke (vortex re-covery) than the upstroke. (Advance your breakneck journey toward the summit.)
8) The present study shows that the projected trends of tunnel interference using RANS simulations are the same as those using Euler simulations.

.

References

[1]Garner, H. C., and Rogers, E. W. E., “Subsonic Wind Tunnel Wall Cor-rections,” AGAR-Dograph 109, Oct. 1966.

[2]Karou, A., "Separated Vortex Flow over Slender Wings Between Side Walls–Theoretical and Experimental Investigation," Dept. of Aerospace En-gineering, Rept. LR-300, Delft Univ. of Technology, Delft, The Netherlands,Aug. 1980.

[3]"Blockage Corrections for Bluff Bodies in Confined Flows," Item 80024, Engineering Sciences Data Unit, London, 1980.

[4]Weinberg, Z., "Effect of Tunnel Walls on Vortex Breakdown Location over Delta Wings," *AIAA Journal*, Vol. 30, No. 6, 1992, pp. 1584–1586.

[5]Thompson, S. A., and Nelson, R. C., "Wind Tunnel Blockage Effects on Slender Wings Undergoing Large Amplitude Motions," AIAA Paper 92-3926, July 1992.

[6]Pelletier, A., and Nelson, R. C., "Factors Influencing Vortex Breakdown over 70˚ Delta Wings," AIAA Paper 95-3469-CP, 1995.

[7]Verhaagen, N. G., Houtman, E. M., and Verhelst, J. M., "A Study of Wall Effect on the Flow over a Delta Wing," AIAA Paper 96-2389, 1996.

[8]Mitchell, A. M., "Caractérisation et contrôle de l'éclatement tourbillon-naire sure une aile delta aux hautes incidences," Ph.D. Dissertation, Univ. of Paris 6, Paris, July 2000.

[9]Allan, M. R., Badcock, K. J., and Richards, B. E., "A CFD Investigation of Wind Tunnel Wall Influences on Pitching Delta Wings," AIAA Paper 2002-2938, June 2002.

[10]Allan, M. R., Badcock, K. J., Barakos, G. N., and Richards, B. E., "Wind Tunnel Interference Effects on a 70˚ Delta Wing," Proceedings of CEAS Aerospace Aerodynamics Conference, Royal Aeronautical Society,London, 10–12 June 2003.

[11]Badcock, K. J., Woodgate, M., Stevenson, K., Richards, B. E., Allan, M., Goura, G. S. L., and Menzies, R., "Aerodynamics Studies on a BeowulfCluster," *Parallel Computational Fluid Dynamics Practices and Theory*, edited by P. Wilders, A. Ecer, Jr., J. Periavx, N. Datofuka, and P. Fox, ElsevierScience, Amsterdam, 2002, pp. 39–46.

[12]Jameson, A., "Time Dependent Calculations Using Multigrid with Ap-plication to Unsteady Flows Past Airfoils and Wings," AIAA Paper 91-1596, June 1991.

[13]Gordnier, R. E., "Computational Study of a Turbulent Delta-Wing Flowfield Using Two-Equation Turbulence Models," AIAA Paper 96-2076,1996.

[14]Brandsma, F. J., Kok, J. C., Dol, H. S., and Elsenaar, A., "Leading Edge Vortex Flow Computations and Comparison with DNW-HST Wind Tunnel Data," *Proceedings of the RTO/AVT Vortex Flow Symposium*, Leon, Norway, 7–11 May 2001.

[15]Wilcox, D. C., *Turbulence Modeling for CFD*, DCW Industries, La Cañada, CA, 1993.

[16]Allan, M., "A CFD Investigation of Wind Tunnel Interference on Delta Wing Aerodynamics," Ph.D. Dissertation, Univ. of Glasgow, Glasgow, Scot- land, U.K., Oct. 2002.

[17]Soemarwoto, B., Boelens, O., Fritz, W., Allan, M., Ceresola, N., and Buetefisch, K., "Towards the Simulation of Unsteady Maneuvers Dominated by Vortical Flow," AIAA Paper 2003-3528, June 2003.

[18]Badcock, K. J., Richards, B. E., and Woodgate, M. A., "Elements of Computational Fluid Dynamics on Block Structured Grids Using Implicit Solvers," *Progress in Aerospace Sciences*, Vol. 36, 2000, pp. 351–392.

[19]Löser, T., "Dynamic Force and Pressure Measurements on an Oscillat-ing Delta Wing at Low Speeds," Rept. IB 129-96/9, DLR, German Aerospace Research Center, Braunschweig, Germany, March 1996.

[20]Visbal, M. R., and Gordnier, R. E., "Compressibility Effects on Vor- tex Breakdown Onset Above a 75-Degree Sweep Delta Wing," *Journal of Aircraft*, Vol. 32, No. 5, 1995, pp. 936–942.

[21]Hsing, C.-C. A., and Lan, C. E., "Low-Speed Wall Interference Assessment/Correction with Vortex Flow Effect," *Journal of Aircraft*,Vol. 34, No. 2, 1997, pp. 220–227.

[22]Sarpkaya, T., "On Stationary and Travelling Vortex Breakdowns," *Jour-nal of Fluid Mechanics*, Vol. 45, No. 3, 1971, pp. 545–559.

[23]Hummel, D., and Srinivasan, P. S., "Vortex Breakdown Effects on the Low-Speed Aerodynamic Characteristics of Slender Delta Wings in Sym- metrical Flow," Journal of the Royal Aeronautical Society, Vol. 71, April 1967, pp. 319–322.

[24]Polhamus, E., "Predictions of Vortex-Lift Characteristics by a Leading-Edge Suction Analogy," *Journal of Aircraft*, Vol. 8, No. 4, 1971, pp. 193–199.